

HQ GRANT  
IN-90-CR

**THEORETICAL STUDIES OF MASS LOSS AND  
SHOCK PHENOMENA IN COOL STAR ENVELOPES**

Grant NAGW-511

Semiannual Progress Reports No. 9 & 10

For the period 1 October 1987 through 30 September 1988

Principal Investigator

Dr. Lee Hartmann

September 1988

Prepared for  
National Aeronautics and Space Administration  
Washington, D.C. 20546

Smithsonian Institution  
Astrophysical Observatory  
Cambridge, Massachusetts 02138

The Smithsonian Astrophysical Observatory  
is a member of the  
Harvard-Smithsonian Center for Astrophysics

The NASA Technical Officer for this grant is Dr. R. V. Stachnik - Code EZ, Headquarters, National Aeronautics and Space Administration, Washington, D.C. 20546.

NASA-CR-1827(8) THEORETICAL STUDIES OF  
MASS LOSS AND SHOCK PHENOMENA IN COOL STAR  
ENVELOPES Semiannual Progress Reports No. 9  
and 10, 1 Oct. 1987 - 30 Sep. 1988  
(Smithsonian Astrophysical Observatory)

N89-13375

Unclas  
G3/90 0167384

## Semiannual Report for NAGW-511

### Disks and Winds in Young Stars

#### *a) Wind-Disk Interactions*

Our paper on physical models for the winds of T Tauri stars has been accepted by the *Astrophysical Journal* (Hartmann and Raymond 1989).

#### *b) Disks in T Tauri stars*

The low-mass, pre-main sequence T Tauri stars exhibit large excesses of infrared emission from warm dust grains ( $T \sim 100$  K to 1500 K). This material must extend close to the star to explain the high dust temperatures and have a large radial extent to produce a range of temperatures, yet there must be relatively clear lines of sight to the stellar photospheres of these objects. A simple way to deal with the observations is to assume that the dust is in a disk around the young star rather than a series of spherical shells. Several other lines of evidence indicate that most young stars are surrounded by dusty disks, including direct observations of extended emission (Beckwith *et al.* 1984; Grasdalen *et al.* 1984). The general blue-shift of forbidden line emission in many young stars has been attributed to occultation of receding material by an opaque disk (Appenzeller, Jankovics, and Ostreicher 1984), and bipolar flow models satisfactorily account for the observed line profiles (Edwards *et al.* 1987).

Adams and Shu (1986) pointed out that a flat, dusty disk will absorb and reprocess  $\sim 25\%$  of the photons emitted by the central star, and Adams, Lada, and Shu (1987) later applied this idea to explain the infrared (IR) energy distributions of pre-main sequence stars. Adams, Lada, and Shu noted that the observed IR excesses are considerably larger than 25% of the stellar flux, suggesting that some of the excess might be produced by a flow of material

through the disk (i.e., accretion).

We have analyzed spectral energy distributions of T Tauri stars to place limits on the amount of accretion which might occur during this early phase of stellar evolution (Kenyon and Hartmann 1987, KH). The typical system has a far-IR energy distribution which follows  $\lambda F_{\lambda} \propto \lambda^{-0.7}$ , while the flat disk model predicts  $\lambda F_{\lambda} \propto \lambda^{-1.3}$ . If the height of the disk photosphere increases faster than linearly with radius (i.e., the disk "flares"), then the energy distribution of a typical T Tauri star will be flatter than  $\lambda F_{\lambda} \propto \lambda^{-1.3}$  because disk annuli at large radii from the central star can absorb more photons. A physically plausible amount of flaring results in an energy distribution which matches the observations of the typical system.

Possibly important uncertainties in these calculations are the assumptions that the disk absorbs all of the photons incident upon it and radiates as a blackbody at the local equilibrium temperature. To address these issues, we have determined the temperature distribution of a dust layer in radiative equilibrium heated from above by radiation obliquely falling on the surface. We illuminated a plane-parallel slab of dust with radiation from a 4000 K star at inclinations and distances appropriate for a flat dusty disk having an outer radius of 1000 times the stellar radius,  $R_*$ . The disk was divided into 16 annuli equally spaced in log radius.

The dust opacity used to calculate the emergent radiation field is an important ingredient for the radiative transfer models. The opacity depends on the composition and size distribution of grains, which are very uncertain in the conditions expected for a circumstellar disk. For our first calculation, we have assumed that the grains are similar in composition and optical properties to grains found in the interstellar medium. We adopted results summarized by Savage and Mathis (1979) for wavelengths below 9000 Å and those of Hildebrand (1984) for  $\lambda > 27 \mu\text{m}$ . At intermediate wavelengths,  $\lambda \sim 1\text{--}27 \mu\text{m}$ , we used the results of Jones and Merrill (1976), scaled to Savage and Mathis at 9000 Å. In this

calculation, the opacity does not depend on the disk temperature.

Our initial results are summarized in Figure 1. The bottom panel of Figure 1 shows the radial temperature distribution expected for a blackbody disk (solid line; from KH) and that determined from the radiative transfer calculation (dotted line). The radiative transfer result is defined as  $T(\tau_\lambda = 2/3)$ , where  $\lambda$  is the wavelength at which  $F_\lambda$  is a maximum. It is apparent that the blackbody temperature is a good approximation for most radii, but begins to fail for  $\log R/R_* \geq 2$ . At these large disk radii, the expected temperature is such that the Planck function peaks at a wavelength where the disk is nearly optically thin. The disk does not emit much radiation at these long wavelengths,  $\lambda > 60 \mu\text{m}$ , so the peak of the energy distribution shifts to shorter wavelengths. At these wavelengths, the disk is optically thick and the radiation temperature is higher than predicted by the simple models.

The flux distribution of the star plus model disk is compared to the blackbody model in the top panel of Figure 1. The blackbody is a fairly good approximation, but it tends to produce more long wavelength flux than the radiative equilibrium calculation. The small excess of radiation relative to the blackbody calculation at  $1 \mu\text{m}$  is a result of stellar flux *scattered* off the disk. At longer wavelengths, the new calculation has a deficiency of flux compared to the blackbody, because of optical depth effects.

Our initial results suggest that energy distributions for circumstellar disks are reasonably well-approximated by the optically thick blackbodies used in our original calculations. In the next year, we plan to see how sensitive the results are to inclination angle in the disk and changes in the opacity law. These radiative transfer solutions will give us a better quantitative understanding of reprocessing disks surrounding T Tauri stars. Constraints on the amount of far-IR flux that can be produced by reprocessing disk models will provide important limits on the necessity for normal viscous accretion in the majority of TTS and for the non-viscous transport of mass and angular momentum as a solution to the peculiar far-IR

energy distributions of several T Tauri stars.

### *c) T Tauri Stars in the HR Diagram*

The Hertzsprung-Russell diagram has been a basic tool for understanding of how single stars evolve once they are on the main sequence. Results for TTS are more ambiguous, because it has been difficult to estimate the luminosity and effective temperatures of the stellar photospheres in these objects. Most TTS display significant infrared and ultraviolet excess radiation over the energy produced by a normal stellar photosphere, and recent results suggest that this radiation is produced by a circumstellar disk which surrounds the star. This extra radiation source complicates estimates of the intrinsic stellar luminosity and the interpretation of the HR diagram.

We have nearly completed a study to assess the uncertainties disks introduce in assigning luminosities and effective temperatures to TTS. An obvious problem with placing a disk around a star is that the disk occults a portion of the stellar hemisphere when the system is viewed at an inclination other than pole-on. Even if the disk did not emit any radiation itself, the apparent stellar luminosity,  $L_{app} = 4 \pi d^2 F$  - where  $d$  is the distance and  $F$  is the bolometric flux received at earth, will be smaller than the true luminosity,  $L_*$ , when the disk inclination is  $i \neq 0^\circ$ . The addition of possible accretion luminosity complicates estimating the predicted distribution of  $L_{app}$  assuming all TTS have the same  $L_*$ .

Our approach to this problem is to predict the distribution of  $L_{app}$  assuming that all TTS have the same intrinsic luminosity,  $L_*$ ; TTS are randomly distributed in inclination,  $i$ ; and TTS have some accretion luminosity,  $L_{acc}$ . We have constructed a sequence of model energy distributions for TTS, following methods outlined by KH. These models consider three radiation sources: a star having mass,  $M_*$ , radius,  $R_*$ , and temperature,  $T_*$ ; a *steady-state* disk, in which the accretion rate,  $\dot{M}$ , is constant with radius through the disk; and a geometrically

thin *boundary layer*, where disk material rotating at Keplerian velocities loses kinetic energy and comes to rest on the slowly-rotating central star.

Preliminary two-dimensional hydrodynamic calculations indicate that it is reasonable to consider the boundary layer as a ring of width  $fR_*$  and scale height  $H_{bl}$  ( $f \ll 1$ ;  $H_{bl} \ll R_*$ ) with  $f \approx H_{bl}/R_*$ . We assume that the region can be characterized by a single effective temperature,  $T_{bl}$ , and density,  $n_{bl}$ . The boundary layer density formally is  $n_{bl} \sim \Sigma_{max}/2H_{bl}$ , but  $\Sigma_{max}$  is sensitive to the choice of the viscosity parameter,  $\alpha$ , and the mass accretion rate,  $\dot{M}$ . We have chosen to determine the boundary layer structure from the energy conservation and continuity equations:

$$\frac{GM_*\dot{M}}{2R_*} = 4\pi f R_*^2 \int_0^\infty \pi B_\lambda(T_{bl}) [1 - e^{-\tau_\lambda(T_{bl})}] d\lambda, \quad (1)$$

$$n_{bl} = \frac{\dot{M}}{4\pi v_R \mu m_H R_* H_{bl}}, \quad (2)$$

where  $v_R$  is the radial drift velocity through the boundary layer and  $\tau_\lambda$  is the optical depth. KH adopted  $v_R = 1 \text{ km s}^{-1}$  as a compromise between the local sound speed  $\sim 10 \text{ km s}^{-1}$  and the drift velocity in the disk  $\sim 0.1 \text{ km s}^{-1}$ , and this seems to be a reasonable assumption until the dependence of  $\Sigma_{max}$  and other physical variables in the boundary layer on assumptions concerning the viscosity are understood.

The “structure equations” for the boundary layer cannot be solved exactly for  $H_{bl}$ ,  $n_{bl}$ , and  $T_{bl}$  unless the region is optically thick at all wavelengths. We adopted initial guesses for these variables assuming the optically thick limit and applied a Newton-Raphson technique to determine self-consistent values. The procedure typically converges in 2-3 iterations and solves equation (1) to  $\sim 0.001\%$ .

As in KH, we assume that the *disk* can be considered as a collection of concentric, optically thick annuli, each of which radiates as a blackbody having an effective temperature,

$T_d$ . The flux emitted by each annulus is the sum of stellar energy absorbed and reprocessed by the annulus,  $F_R$ , and the energy liberated by viscous stresses within the disk (i.e., the accretion energy),  $F_A$ . The effective temperature is computed according to the blackbody relation,  $T_d^4(R) = [F_A(R) + F_D(R)]/\sigma$ .

A sample model optical spectrum is compared to dereddened optical spectrophotometry of GG Tau in Figure 2. The model in the top panel of the Figure is for an accretion rate of  $\dot{M} = 5.2 \times 10^{-8} M_\odot \text{ yr}^{-1}$  onto a pre-main sequence star with a radius of  $3 R_\odot$ , a mass of  $0.5 M_\odot$ , and an effective temperature of 3750 K. The model has been scaled to a distance of 160 pc to compare with the data for GG Tau in the bottom panel. The observations of GG Tau have been corrected for a modest amount of interstellar reddening ( $A_V \sim 0.5 \text{ mag}$ ).

It is apparent that the model adequately accounts for several features observed in GG Tau, including the height of the Balmer jump and the depths of several absorption bands. We have not tried to determine a “best-fit” to the data in the least-squares sense, but plan to develop software for this task over the next several months.

To construct a theoretical H-R diagram for TTS, we have calculated spectral energy distributions for a variety of accretion rates  $\dot{M}$  through a disk surrounding an M0 pre-main sequence star with a radius of  $3 R_\odot$  and a luminosity of  $1.6 L_\odot$ . We characterize each calculation by the amount of “veiling” accretion produces at  $5550 \text{ \AA}$ ,  $r$ , as a function of the inclination,  $i$ . The veiling parameter,  $r$ , is defined as the fraction of flux at  $5550 \text{ \AA}$  supplied by the disk and the boundary layer and ranges from 0 (no veiling) to 1 (complete veiling). The “stellar luminosity” of each model is estimated by normalizing the energy distribution of an M0 star to the calculated energy distribution at V, R, I, J, and K. This allows us to calculate the ratio of the inferred luminosity,  $L$ , to the true stellar luminosity,  $L_*$ , at each wavelength, for a range of inclinations,  $i$ , and veiling,  $r$ .

If we assume that TTS are oriented randomly in space, then the probability density of TTS having  $\log (L/L_*)$  is:

$$p(\log L/L_*) = \int_0^{0.75} n(r) A(r) \frac{L}{L_*} dr , \quad (3)$$

where  $A(r)$  is a normalization constant.

To compare the expression for  $p(\log L/L_*)$  with observations of TTS requires some knowledge of the errors introduced in estimating  $\log (L/L_*)$  from the data. Obvious sources of error include the distance, the interstellar extinction, and the spectral type, and our estimates for these are listed in Table 1. These results have been added in quadrature to produce a total error,  $\sigma(\log L/L_*)$ , which is listed in the final column of Table 1. The uncertainty in the luminosity is smallest in I and J,  $\sim 0.1$  in  $\log (L/L_*)$ , and is severe for V,  $\sim 0.2$  in  $\log (L/L_*)$ .

Table 1  
Luminosity Dispersions for T Tauri Stars

Wavelength	Distance	Extinction	Spectral Type	Total
V	0.058	0.186	0.064	0.205
I	0.058	0.090	0.045	0.116
J	0.058	0.052	0.073	0.107

We assume that the error in  $\log (L/L_*)$  is distributed randomly, and thus convolve the theoretical distribution for  $p(\log L/L_*)$  with a gaussian of width  $\sigma(\log L/L_*)$  for comparison with the data. The final distribution is then:

$$P(\log L/L_*) = \int_0^{\infty} p(\log l/l_*) e^{-[(\log l/l_* - \log L/L_*)/\sigma]^2} d\log l/l_* , \quad (4)$$

Several examples of predicted probability densities are presented in Figure 3. The two lefthand panels show  $P(\log L/L_*)$  for models in which the veiling flux is 0% ( $r = 0$ ) and 50% ( $r = 0.5$ ) of the stellar luminosity at 5550 Å. When the accretion luminosity is small (i.e.,



when  $r$  is close to zero), most of the disk luminosity is produced by reprocessing and the apparent stellar luminosity is close to the true stellar luminosity. The apparent luminosity greatly exceeds  $L_*$  when accretion is a significant luminosity source, as shown in the upper left panel of Figure 3.

It is not possible to predict the distribution of accretion rates,  $\dot{M}$ , among TTS, so we have estimated the amount of veiling directly from observations of TTS. The observations are consistent with TTS having a roughly uniform distribution of veiling from  $r \sim 0$  to  $r \sim 0.5$  with a few extra TTS having  $r \sim 0.5$  to  $0.75$ . We have considered two cases: (i)  $n(r) =$  constant from  $r = 0$  to  $r = 0.5$ , and (ii)  $n(r) = 0.75 - r$ , for  $0 \leq r \leq 0.75$ . Our results are displayed in the right panels of Figure 3, and it is obvious that the predicted probability distributions are not sensitive to the form of the veiling distribution.

The models suggest that the combined effects of accretion and disk inclination would produce a measurable spread in the observed luminosities of TTS even if the underlying stars all had the same luminosity,  $L_*$ . The width of the distribution is sensitive to the wavelength at which  $L_*$  is estimated. We found that the minimum width occurs for the I and J bandpasses, so these wavelengths provide the best estimate for the stellar luminosity of a given TTS. Large dispersions in  $L/L_*$  result at V and K, and these bandpasses should not be used to estimate the stellar luminosity of a TTS.

The width of the probability distribution provides a useful estimate of the minimum age spread which can be measured in a T association. The luminosity of a star contracting to the main sequence along the Hayashi track follows  $L \sim 1 (t/3 \times 10^5 \text{ yr})^{-2/3} L_\odot$ , so the minimum age spread which can be inferred from observations of  $L$  is  $\sim 1\text{-}2 \times 10^6 \text{ yr}$ .

We have estimated the stellar luminosities,  $L(J)$ , of TTS using published J magnitudes and extinctions, and have plotted the results as a histogram in Figure 4. The width of the observed distribution is significantly larger than that of the predicted distribution. An age

spread of  $\sim 3 \times 10^6$  yr is sufficient to explain the width of the observed distribution in L(J).

We plan to complete this project over the next several months. These results have an obvious impact on the stellar birthline proposed by Stahler (1983) and one of our goals is to explore the statistical significance of the birthline for TTS. In addition, Walter *et al.* (1987) have discovered a class of pre-main sequence stars, the weak-lined TTS, which appear to lack (or possess minimal) ultraviolet and infrared excesses. Our analysis may make it possible to compare the luminosity functions for the classical and weak-lined TTS and determine if the weak-lined objects are TTS in which the disk has dispersed or whether some process has prevented the formation of disks around these stars.

## References

- Adams, F.C., Lada, C.J., and Shu, F.H. 1987, *Ap. J.*, **312**, 788.  
Adams, F.C., and Shu, F.H. 1986, *Ap. J.*, **308**, 836.  
Appenzeller, I., Jankovics, I., and Ostreicher, R. 1984, *Astr. Ap.*, **141**, 108.  
Beckwith, S., Zuckerman, B., Skrutskie, M.F., and Dyck, H.M. 1984, *Ap. J.*, **287**, 793.  
Edwards, S., Cabrit, S., Strom, S.E., Heyer, I., and Strom, K.M. 1987, *Ap. J.*, **321**, 473.  
Grasdalen, G.L., Strom, S.E., Strom, K.M., Capps, R.W., Thompson, D., Castelaz, M. 1984, *Ap. J. (Letters)*, **283**, L57.  
Hildebrand, R.H. 1984, *Q.J.R.A.S.*, **24**, 267.  
Jankovics, I., Appenzeller, I., and Krautter, J. 1983, *Pub. Astron. Soc. Pacific*, **95**, 883.  
Jones, T.W., and Merrill, K.M. 1976, *Ap. J.*, **209**, 509.  
Kenyon, S.J., and Hartmann, L. 1987, *Ap. J.*, **323**, 714.  
Lynden-Bell, D., and Pringle, J.E. 1974, *Mon. Not. Roy. Astr. Soc.*, **168**, 603.  
Savage, B.D., and Mathis, J.S. 1979, *Ann. Rev. Astr. Ap.*, **17**, 73.

**Publications**

Hartmann, L., and Raymond, J.C. "Wind-Disk Shocks Around T Tauri Stars," *Ap. J.*, in press (1989).

### Figure Captions

Figure 1 - Comparison of predicted temperature (lower panel) and energy distributions (upper panel) for a blackbody disk (solid lines) and the radiative transfer calculation (dotted lines). The temperature at  $\tau = 1$  in the transfer calculation follows the blackbody model until the disk becomes optically thin at far-IR wavelengths.

Figure 2 - top panel: model energy distribution for a TTS with an optically thin boundary layer. bottom panel: observed energy distribution of GG Tau, a moderately veiled TTS.

Figure 3 - Predicted luminosity functions for T Tauri stars.

Figure 4 - Comparison of the observed distribution of TTS luminosities with predictions of the disk models describe din the text.

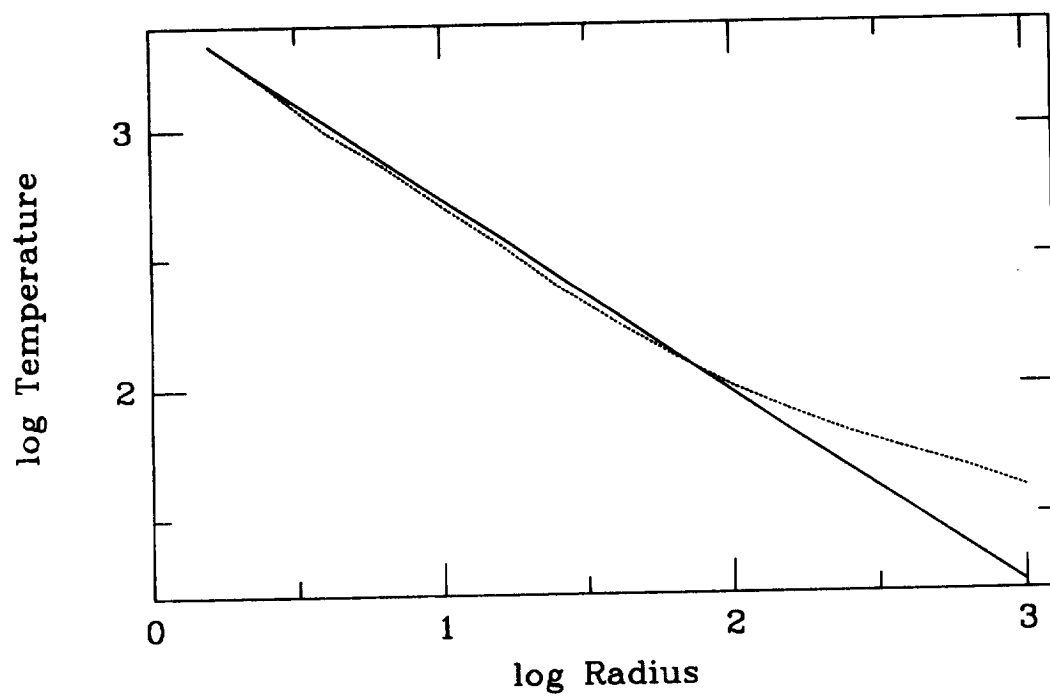
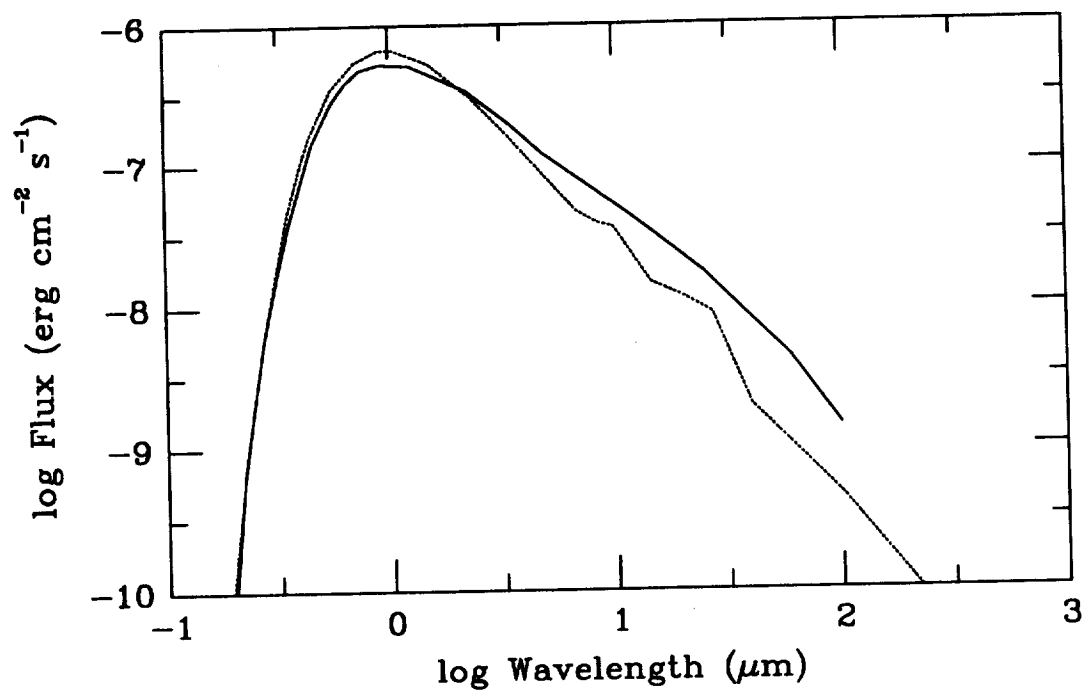


Figure 1

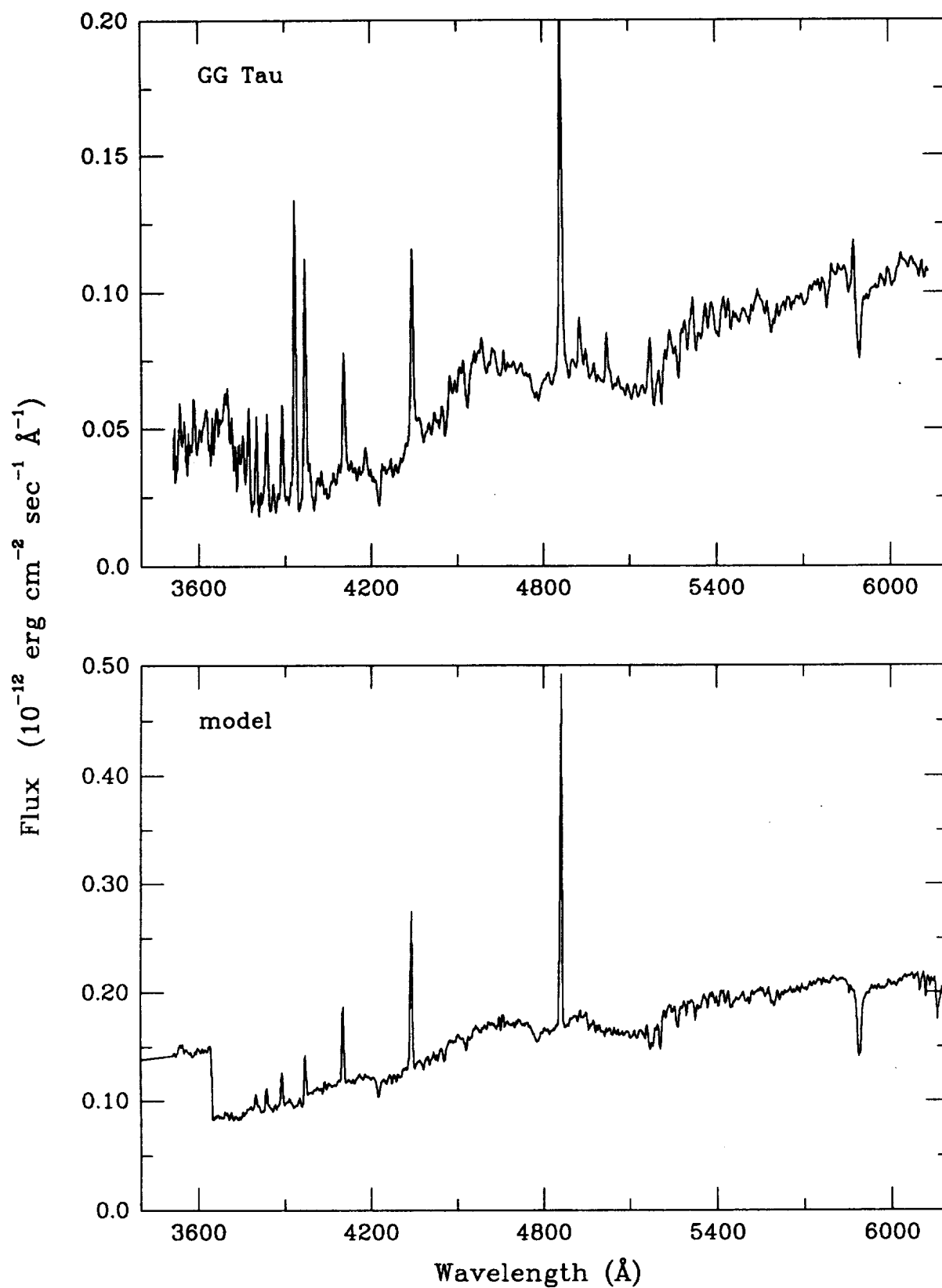


Figure 2

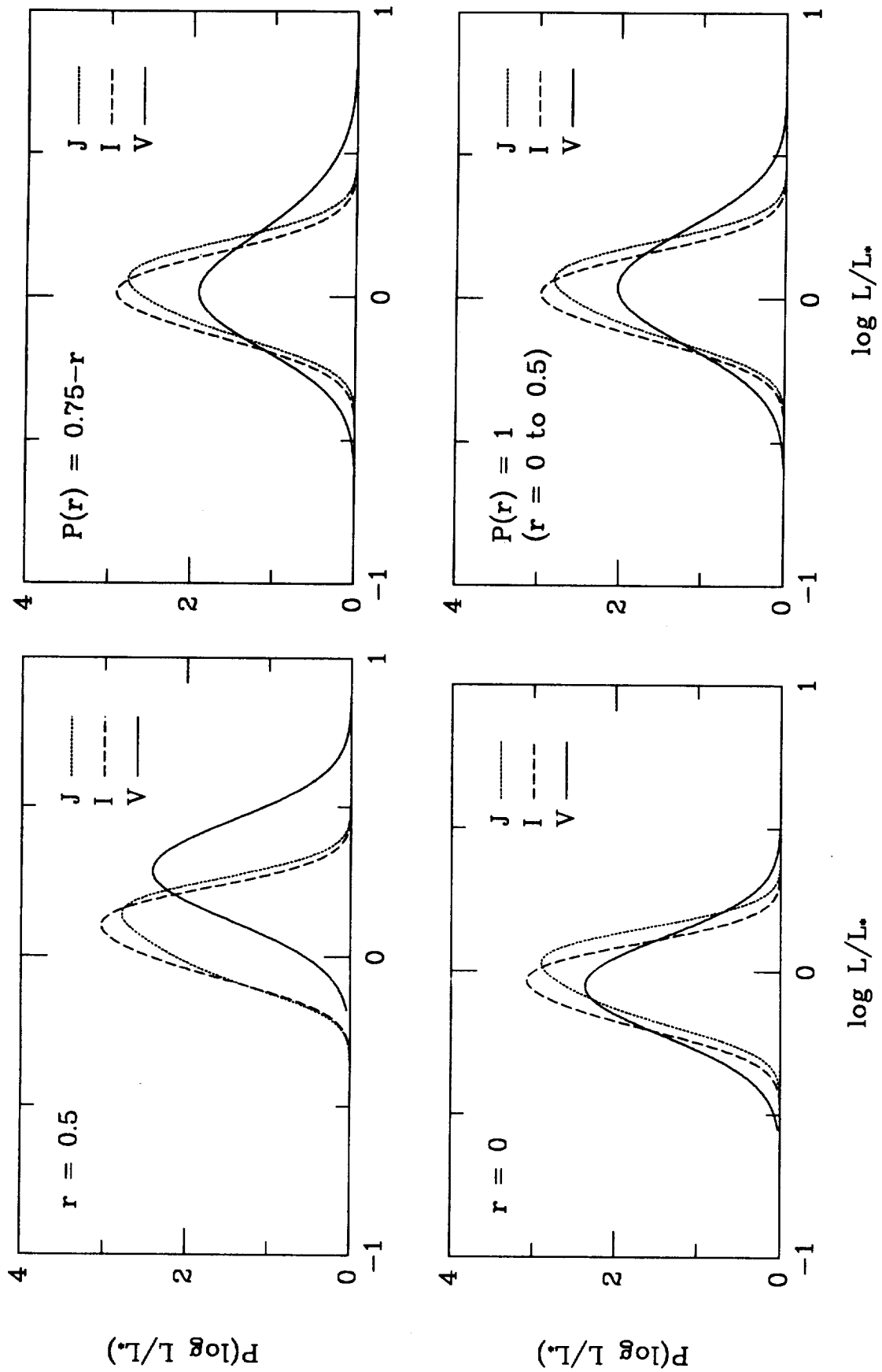


Figure 3



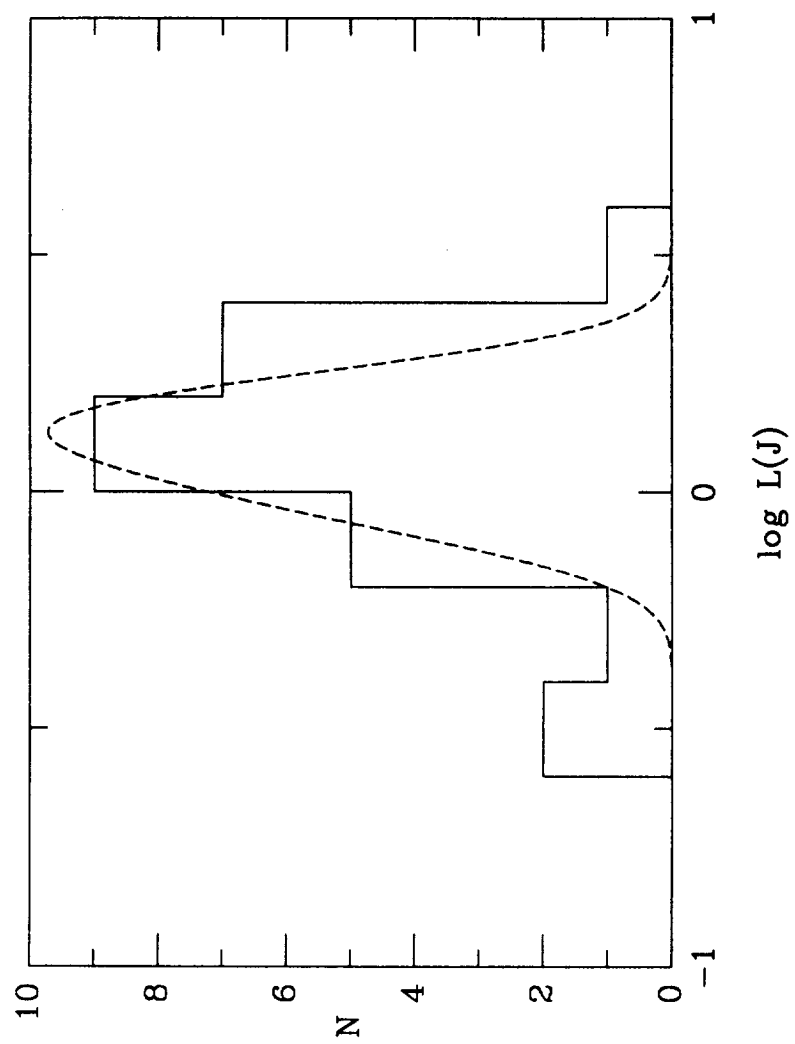


Figure 4